

Black Carbon Increases Cation Exchange Capacity in Soils

B. Liang, J. Lehmann,* D. Solomon, J. Kinyangi, J. Grossman, B. O'Neill, J. O. Skjemstad, J. Thies, F. J. Luizão, J. Petersen, and E. G. Neves

In Memory of James Petersen

Dr. James Petersen was killed during an armed robbery while doing research near Manaus, Brazil, on 13 Aug. 2005. Dr. Petersen was associate professor and chair of the Anthropology Department at University of Vermont. We will miss him as a valued colleague and good friend.

ABSTRACT

Black Carbon (BC) may significantly affect nutrient retention and play a key role in a wide range of biogeochemical processes in soils, especially for nutrient cycling. Anthrosols from the Brazilian Amazon (ages between 600 and 8700 yr BP) with high contents of biomass-derived BC had greater potential cation exchange capacity (CEC measured at pH 7) per unit organic C than adjacent soils with low BC contents. Synchrotron-based near edge X-ray absorption fine structure (NEXAFS) spectroscopy coupled with scanning transmission X-ray microscopy (STXM) techniques explained the source of the higher surface charge of BC compared with non-BC by mapping cross-sectional areas of BC particles with diameters of 10 to 50 μm for C forms. The largest cross-sectional areas consisted of highly aromatic or only slightly oxidized organic C most likely originating from the BC itself with a characteristic peak at 286.1 eV, which could not be found in humic substance extracts, bacteria or fungi. Oxidation significantly increased from the core of BC particles to their surfaces as shown by the ratio of carboxyl-C/aromatic-C. Spotted and non-continuous distribution patterns of highly oxidized C functional groups with distinctly different chemical signatures on BC particle surfaces (peak shift at 286.1 eV to a higher energy of 286.7 eV) indicated that non-BC may be adsorbed on the surfaces of BC particles creating highly oxidized surface. As a consequence of both oxidation of the BC particles themselves and adsorption of organic matter to BC surfaces, the charge density (potential CEC per unit surface area) was greater in BC-rich Anthrosols than adjacent soils. Additionally, a high specific surface area was attributable to the presence of BC, which may contribute to the high CEC found in soils that are rich in BC.

BIO MASS-DERIVED BC exists ubiquitously in soils to varying extents as a result of deliberate vegetation burning, wild fires or energy production (Schmidt and Noack, 2000). Black C is also a product of fossil fuel burning and can occur in geological deposits, but these two forms of BC are not considered here. Worldwide BC formation

from biomass burning was estimated to be 50 to 270 Tg yr^{-1} with more than 90% of the BC remaining in terrestrial ecosystems (Kuhlbusch et al., 1996). The majority of BC is believed to be stored in soils (Masiello, 2004), and can constitute a significant fraction of C buried in soils (Skjemstad et al., 1996; Schmidt et al., 1999; Schmidt and Noack, 2000). Black C may play an important role in a wide range of biogeochemical processes, such as adsorption reactions (Schmidt and Noack, 2000). The importance of adsorption of polycyclic aromatic hydrocarbons (PAH) and other organic pollutants to both biomass- and fossil fuel-derived BC in soils and sediments has been established over the past years (Ghosh et al., 2000; Accardi-Dey and Gschwend, 2002; Braida et al., 2003). Limited information is available, however, on the effects of biomass-derived BC on adsorption of base cations in soil.

The chemical structure of BC is highly aromatic (Schmidt and Noack, 2000), yet the possibility of abiotic and microbial oxidation, and the formation of functional groups with net negative charge on BC particle surfaces cannot be ruled out (Schmidt et al., 2002). For example, charred plants showed large amounts of extractable humic and fulvic acids with high concentrations of carboxylic groups after oxidative degradation with dilute HNO_3 (Trompowsky et al., 2005).

Strong evidence suggests that nutrient dynamics in soil can significantly be influenced by BC (Glaser et al., 2001; Lehmann et al., 2003b). Anthrosols rich in BC were found to maintain high cation availability (Lima et al., 2002) compared with adjacent forest soils with similar mineralogy despite high leaching conditions in humid tropical Amazonia. Due to the prevalence of highly weathered clay minerals such as kaolinite in these soils, their ability to retain cations depends entirely on soil organic matter (SOM) contents (Sombroek, 1966). In addition to greater potential CEC associated with greater SOM contents, also trends of significantly higher CEC per unit soil organic C were observed in these Anthrosols compared with adjacent forest soils (Sombroek et al., 1993). Such greater CEC could be created by either of two mechanisms: (i) by a higher charge density per unit surface area which means a higher degree of oxidation of SOM; or (ii) by a higher surface area for cation adsorption sites, or a combined effect of both. Black C enrichment was believed to be the main contributor to the higher CEC in Anthrosols but the mechanism remained unclear (Glaser et al., 2001). Glaser et al. (2003) suggested the oxidation of the aromatic C and formation of carboxyl groups to be the main reason for

B. Liang, J. Lehmann, D. Solomon, J. Kinyangi, J. Grossman, B. O'Neill, and J. Thies, Dep. of Crop and Soil Sciences, Cornell Univ., Ithaca, NY 14853, USA; J.O. Skjemstad, CSIRO Land and Water, Glen Osmond SA 5064, Australia; F.J. Luizão, Instituto Nacional de Pesquisa da Amazônia (INPA), 69011-970 Manaus, Brazil; J. Petersen (deceased), Dep. of Anthropology, Univ. of Vermont, Burlington, VT, 05405 USA; E.G. Neves, Museu de Arqueologia e Etnologia, Universidade de São Paulo, São Paulo, SP, 05508-900, Brazil. Received 28 Nov. 2005. *Corresponding author (CL273@cornell.edu).

Published in Soil Sci. Soc. Am. J. 70:1719–1730 (2006).

Soil Chemistry

doi:10.2136/sssaj2005.0383

© Soil Science Society of America

677 S. Segoe Rd., Madison, WI 53711 USA

Abbreviations: ACU, Açutuba; BC, black carbon; CEC, cation exchange capacity; DS, Donna Stella; HAT, Hatahara; LG, Lago Grande; NEXAFS, near edge X-ray absorption fine structure; NMR, nuclear magnetic resonance; SSA, specific surface area; SOM, soil organic matter; STXM, scanning transmission X-ray microscopy.

the observed high CEC. Such formation of carboxyl groups or other functional groups with net negative charge in the pH range of soils can be the result of two principally different processes: (i) surface oxidation of BC particles themselves; or (ii) adsorption of highly oxidized organic matter onto BC surfaces (Lehmann et al., 2005). To understand the mechanisms involved in the creation of negative surface charges on highly aromatic BC particles, nano-scale distribution of organic C forms have to be studied as most of the BC particles in soils are typically <50 μm in size (Skjemstad et al., 1996).

However, measurements of BC chemical surface properties are rare due to methodological limitations. Most previous studies on the structural characterization of BC relied on destructive methods for the preparative isolation of BC before the chemical characterization, such as thermal, chemical or ultra-violet (UV) oxidative treatments (Skjemstad et al., 1996; Gelinás et al., 2001; Masiello et al., 2002). Such isolation methods fall short of retaining the intact and original chemical properties of the BC particle surfaces. Spectroscopic methods such as high-resolution transmission electron microscopy (TEM) (Palotas et al., 1996), micro-Raman spectroscopy and electron energy loss spectroscopy (EELS) (Schmidt et al., 2002), and scanning electron microscopy (SEM) (Stoffyn-Egli et al., 1997; Fernandes et al., 2003; Brodowski et al., 2005) have been used to study single particles and general BC morphology, surface characteristics and texture, and even nanomorphology features without the necessity of isolating the BC by oxidative techniques. However, none of these techniques allows imaging of the spatial distribution of C forms with sub-micrometer resolution. Novel synchrotron-based STXM coupled with NEXAFS spectroscopy techniques provide unique opportunities for imaging the spatial distribution of organic C forms on BC particle sections with a resolution of up to 50 nm (Lehmann et al., 2005).

Our research objectives were: (1) to investigate the effectiveness of BC for increasing CEC in comparison with non-BC; and (2) to assess the mechanisms by which BC contributes to soil CEC. We hypothesized (i) that BC is more effective than non-BC in creating CEC; (ii) that BC surfaces are oxidized and show large amounts of negatively charged functional groups; and (iii) that BC has a higher surface area than non-BC per unit mass.

MATERIALS AND METHODS

Soil Information

Black C-rich Anthrosols and adjacent soils were sampled from four archaeological sites, Hatahara (HAT), Lago Grande

(LG), Acutuba (ACU) and Dona Stella (DS), near Manaus, Brazil (3°8' S, 59°52' W, 40–50 m above sea level), which have been dated to span from about 600 to 8700 yr (Table 1; modified from Neves et al., 2003; E.G. Neves, unpublished data, 2005). Rainfall is highest between December and May (73% of total annual rainfall) with a mean annual precipitation of 2000 to 2400 mm (Sombroek, 2001). The natural vegetation is tropical lowland rainforest. The studied Anthrosols (locally known as 'Terra Preta de Indio') are the result of pre-Columbian settlements (Sombroek, 1966; Smith, 1980; McCann et al., 2001; Petersen et al., 2001), developed on Oxisols, Ultisols, or Spodosols (USDA, 1999). Lago Grande was covered by an old secondary forest whereas HAT and ACU showed signs of recent agricultural activities and DS was under natural campinarana vegetation. Being the oldest site, the DS Anthrosol showed lithic remains, whereas the other three sites bore ceramic artifacts all indicating pre-Columbian occupation. A wide range of ages was selected for the occupation and therefore creation of the Anthrosols to allow broader statements concerning the nature of BC associated with different lengths of exposure. Sites of adjacent soils were chosen based on maximum color difference between the BC-rich and dark Anthrosols containing artifacts to adjacent soils with typical pale yellow or white soil color without visible signs of human occupation (Table 1). The soil types of adjacent soils ranged from Oxisols (HAT, LG, ACU) to Spodosols (DS) (USDA, 1999). To ensure that the anthropogenic effects were minimal on sites classified as adjacent soils, approximately double the distance between the Anthrosol and the nearest location of a soil with maximum color difference were used for sampling adjacent soils. However, it cannot be ruled out that some anthropogenic impacts may have changed the properties of adjacent soils. For example, the total P concentrations were higher on adjacent soils (Table 1) than on soils under primary forests in the area (Lehmann et al., 2001). But these influences may have been small and still provided a sufficiently large contrast with respect to levels of BC between Anthrosols and adjacent soils. Samples were taken from the entire soil profile according to genetic horizons. Total C and potential CEC are shown for all horizons (Fig. 2). The analyses of BC properties were only done for one horizon per soil type and site due to limitations with the time-consuming spectroscopic measurements. Analyses of adjacent soils were done from the A horizon. For the Anthrosols, however, mostly subsurface horizons below a layer of potshards were used to exclude the possibility of any recent BC inputs for example due to forest burning or anthropogenic activities. All samples were air-dried and large plant debris were removed.

Soil Analyses

Soil samples from each site were sieved to 2 mm, homogenized, and for combustion analyses finely ground using a Mixer Mill (MM301, Retsch, Germany). Subsamples were analyzed for organic C and total N contents with an Europa

Table 1. Chemical properties of selected horizons from BC-rich Anthrosols and adjacent soils in the central Amazon.

Site	Type	Depth cm	Color dry soil	Age yr	Sand Silt Clay			pH		Organic C mg g ⁻¹	Total N	C/N	Total P		Total Ca mg kg ⁻¹
					%	1:2.5 H ₂ O	1:2.5 KCl	mg g ⁻¹	mg kg ⁻¹						
HAT	Anthrosol	43–69	10YR 4/1	600–1000	51.3	21.7	27.0	6.4	5.5	22.0	1.0	23	9064	17545	
	Adjacent soil	0–10	10YR 5/4		60.4	3.8	35.9	4.6	3.8	21.8	1.6	14	273	115	
LG	Anthrosol	0–16	10YR 3/1	900–1100	47.9	29.6	22.6	5.9	4.9	31.5	1.8	18	5026	6354	
	Adjacent soil	0–8	7.5YR 5/4		69.4	3.9	26.7	4.2	3.5	17.5	1.3	14	251	119	
ACU	Anthrosol	48–83	10YR 4/1	2000–2300	81.9	7.7	10.4	5.6	4.2	15.7	1.0	16	777	332	
	Adjacent soil	0–30	7.5YR 4/2		87.9	3.6	8.5	4.7	3.9	15.4	0.8	20	198	50	
DS	Anthrosol	190–210	5YR 3/1	6700–8700	96.8	2.9	0.3	5.0	4.1	16.5	1.1	15	139	40	
	Adjacent soil	0–12	5YR 2/2		91.1	8.6	0.3	3.9	2.6	10.2	0.4	27	51	165	

ANCA GSL sample combustion unit (PDZEuropa, Crewe, England). Soil effective and potential CEC were determined by the BaCl_2 (0.1 M, 20 mL for 2 g soil) compulsive exchange method (Gillman and Sumpter, 1986; Hendershot and Duquette, 1986) and with ammonium acetate (1 M, 2.5 g soil) at pH = 7 (Holmgren et al., 1977; Sumner and Miller, 1996), respectively. The potential CEC and total C were measured on soil samples with and without peroxide digestion to remove non-BC. Twenty grams of air-dried soil were treated with 30% (w/w) peroxide (Mallinckrodt) (initially 10 mL, with daily additions up to a total of 30–50 mL until no further bubbles appeared) and heated on a hot plate at 90°C to ensure maximum non-BC removal.

For analysis of total elemental P and Ca, 0.5 g soil was digested in 9 mL of concentrated nitric and 3 mL hydrofluoric acid for 15 min using a microwave, and quantified by inductively coupled plasma atomic emission spectrometry (ICP-AES, Spectro CIROS, CCD, Germany) according to procedure EPA 3052. Soil texture was determined using the pipette method with 20 g dry soil dispersed in 1000 mL of 10% (w/v) Calgon solution, separated by sedimentation for different periods of time, dried, and weighed (Gee and Or, 2002). The mineralogy of the clay fraction (<0.002 mm, separated by sedimentation) was determined by X-ray diffraction analysis (XRD, Theta-Theta Diffractometer, Scintag Inc., Cupertino, CA) using monochromatic $\text{CuK}\alpha$ radiation on oriented clay samples on glass slides (Whittig and Allardice, 1986). Specific surface area (SSA) was determined by an automated surface area analyzer (ASAP 2020, Micromeritics Instruments Corp., Norcross, GA) with the BET N_2 method (Pennell, 2002). Five to 20 g air-dried and dispersed soil samples were degassed at 90°C until the pressure stabilized at 8 mm Hg, and N_2 was equilibrated at different pressures to obtain thermal adsorption and desorption curves with a total of 169 points. Adsorption data were fitted to a Type IV isotherm.

The proportion of BC as a fraction of total organic C was estimated by two approaches, (i) using nuclear magnetic resonance (NMR) spectroscopy and high energy UV oxidation; and (ii) thermal oxidation by CTO-375. NMR spectra were obtained after removal of soil minerals by 2% (w/v) HF (Skjemstad et al., 1996). Additionally, soils were treated with UV at 2.5 kW for 2 h and remeasured by NMR and dry combustion for organic C (Skjemstad et al., 1996). Black C was expressed as the percentage of organic C following the procedure described by Skjemstad et al. (1999). Additionally, the aromaticity of the HF-treated soils was given as a proportion of the NMR peak area at 110 to 150 ppm. The UV oxidation method captures biomass-derived BC or charcoal as well as more aromatic forms of BC. The thermal method CTO-375, however, quantifies more graphitic BC (Masiello, 2004). For thermal oxidation, 60 mg of dried soil (at 60°C) were weighed into pretared porcelain crucibles with a silica glaze surface (Coors Ceramics, Golden, CO). Samples were combusted in a furnace at 375°C for 24 h in the presence of excess oxygen and reweighed after cooling in a desiccator (Gustafsson et al., 1997). Approximately 20 mg of each cooled sample were weighed into opened pretared Ag capsules (model 8 × 5 mm; Elemental Microanalysis Ltd, Manchester, NH) and demineralized with 1 M HCl until no further effervescence was observed. Capsules were closed and samples were measured for organic C on an Europa ANCA GSL sample combustion unit (PDZEuropa, Crewe, England).

Sample Preparation for NEXAFS and Microprobe

Black C particles (sizes from 10 to 150 μm) were picked from one horizon of each of the four Anthrosols using super

tweezers (N5, Dumont, Montignez, Switzerland) under a light microscope (30×; SMZ-10, Nikon, Japan). After about 40 to 60 particles were obtained from each soil, characteristic particles were selected for further spectroscopic analyses. Carbon-free elemental S (99.9%, Fisher Scientific, Hampton, NH) was used as the embedding material. Detailed sample preparation procedures were given by (Lehmann et al., 2005). In brief, elemental S was heated (220°C) to a polymerized state, immediately molded into a block (diameter of 8 mm, height of 15 mm lined with aluminum foil) and super-cooled. The BC particles were quickly embedded into the elemental S during the brief warm-up and viscous period, and later sectioned using an ultramicrotome (Ultracut UTC, Leica Microsystems Inc., Bannockburn, IL). Sections with a thickness of 100 to 200 nm were obtained with a diamond knife (MS9859 Ultra 45°, Diatome Ltd., Biel, Switzerland) at a cutting speed of 0.3 to 1.2 mm s^{-1} (angle of 6°) and transferred to Cu grids (carbon free, 200 mesh, silicon monoxide No. 53002, Ladd Research, Williston, VT) and air-dried. Before the spectroscopic analyses, S on the sections was sublimed in a vacuum oven (40°C, -31 bars) for 1 h. Two representative BC particles were shown for Anthrosols at HAT, LG, and ACU sites, but only one at the DS site (due to lack of successful sections).

In addition to the BC particles, also a clay particle, humic substances from the adjacent soil at HAT site, fungal hyphae and bacteria were measured. Humic substances were extracted from bulk soil (soil/solution ratio = 1:5 w/v) with a 0.1 M NaOH and 0.4 M NaF mixture at pH = 12.4 under N_2 environment (Solomon et al., 2005). Extracts were filtered (0.2 μm pore size, Gelman Supor; Pall Gelman Laboratory, MI, USA) and dialyzed (Spectra/Por Membrane, MWCO, 12000–14000 Da; Spectrum Laboratories, CA) in distilled water to remove soluble salts, and lyophilized using a freeze dryer (Kinetics Thermal Systems, Stoneridge, NY). Fungal (*Ascomycete* sp.) and bacteria [gram (-) *alphaproteobacteria*] colonies were pre-isolated from Anthrosols (HAT site, 43- to 69-cm depth) and cultivated in potato dextrose broth (24 g L^{-1} tap) and LB broth (Bacto peptone 10 g, yeast extract 5 g, NaCl 5 g L^{-1}), respectively, which were distributed into 5 mL volumes in screw top tubes and sterilized for 15 min at 121°C. One milliliter of culture of fungi (after 5 d, 37°C) and bacteria (after 24 h, 37°C) were transferred into eppendorf tubes and centrifuged at 5000 rpm for 5 min, and sequentially washed with 0.05 M NaCl twice after discarding the supernatant. Samples were resuspended in 0.5 mL of saline water and kept on ice until measurement. An aliquot of 10- μL sample was dispersed on silicone monoxide Cu-grids and air-dried before mounting to the STXM.

STXM and NEXAFS Data Collection and Analysis

Coupled with STXM, NEXAFS images were recorded at different energies below and above the C absorption K edge (284.3 eV) at the X1-A endstation of the National Synchrotron Light Source at Brookhaven National Laboratory. The synchrotron beam delivers a flux of $\sim 10^7$ photons s^{-1} , with an energy bandwidth of about 0.1 eV for the soft X-ray. Due to difficulties in maintaining the sample at the focal distance for submicrometer-sized areas, direct recording of NEXAFS data by simple scanning of the incident radiation energy at fixed sample position was not possible. Therefore, a Fresnel zone plate focus was used and stack images were recorded to overcome this limitation (Rothe et al., 2000). Energy increments were set from 280 to 282.5 eV at 0.3 eV (dwell time 1 ms), up to 292 at 0.1 eV (dwell time 3 ms), and up to 310 eV at 0.3eV (dwell time 3 ms). One image was taken by each x-y scanning of a selected sample area. Individual images scanned at all

energy levels were stacked using the Stack-Analyze software (C. Jacobsen, SUNY Stony Brook; built on IDL software, Research Systems Inc., Boulder, CO). Then a mathematical alignment procedure (using 290 eV as a constant reference) was performed to correct for the mechanical shift of the sample stage out of the focus spot (<0.3 pixels). Spectra of selected sample regions can be extracted by vertical projections of corresponding zones on collected stacks. After defining a background correction area (I_0), principal component and cluster analyses were performed with PCA_GUI 1.0 (Lerotic et al., 2004) to classify sample regions with similar spectral characteristics after orthogonalizing and noise-filtering the data. Different numbers of components and clusters were used to test the robustness of the results. A combination of two to five components and four to six clusters yielded the lowest errors. Singular value decomposition (SVD) was calculated to obtain target maps and associated target spectra (Lehmann et al., 2005).

Microprobe Elemental Analysis

Microprobe analysis (JEOL_JXA-8900, Pioneer, Japan) with five crystal spectrometers (WDS, Thermo Electron Corp, Middleton, WI) was explored to map the spatial distribution of selected elemental contents (C, O, Cl, K) over BC cross-sections, coupled with a Vantage analyzer. A Si(Li) detector with a thin window was used to detect light elements such as C (Stoffyn-Egli et al., 1997). The instrument was set to an accelerating voltage of 10.00 KeV, and generated a current of 1.98×10^{-8} Amp. Sample measuring live time was 30 s, with a take-off angle of 40° under $1500\times$ magnification.

Statistical Analyses

Linear regressions and *t* tests were done using Statistica 5.1 (StatSoft, Hamburg, Germany).

RESULTS AND DISCUSSION

Soil Properties

Soil texture and mineralogy of the clay fraction determined by sedimentation and XRD revealed that Anthrosols and adjacent soils were of similar mineralogical characteristics and origin, with predominantly 1:1 kaolinitic clay, while no 2:1 diffraction peaks such as from vermiculite were identified (Fig. 1). However, Anthrosols had much higher total P (3–33 times) and Ca (7–153 times, except in the oldest Anthrosol DS), and pH than adjacent soils (Table 1). These features indicate a higher fertility in Anthrosols than adjacent soils that are characteristic of these anthropogenic soils (Lehmann et al., 2003a).

The organic C contents were found to be rather similar between the selected horizons of Anthrosols and adjacent soils studied here (Table 1; apart from LG). This was largely an effect of the specific sample selection and does not reflect typical differences between Anthrosols and adjacent soils. This approach aided in an unambiguous interpretation of the C quality, as the Anthrosol samples contained a higher proportion of BC. Solid state ^{13}C CP/MAS NMR analysis after UV treatment indicated a BC increase from below detection limit of 1.5 to 51% of total organic C from adjacent soil to Anthrosol at LG (Table 2). Nuclear magnetic resonance spectroscopy

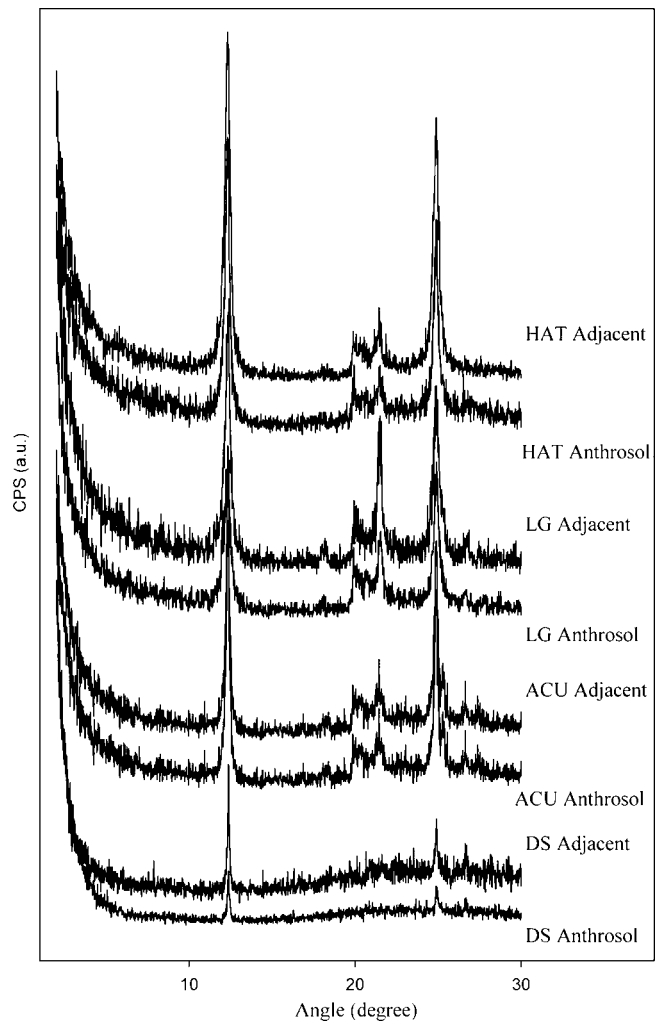


Fig. 1. X-ray diffraction (XRD) analysis of the clay fraction, identified peak pattern fits into aluminum silicate hydroxide/Kaolinite-1A, which is the dominant mineral.

copy of unoxidized samples showed that Anthrosols contained SOM with 55 to 238% higher levels of aromaticity than adjacent soils (Table 2), which was calculated as the ratio of total aromatic C in the spectral region 110 to 150 ppm to total C in the spectral region 0 to 230 ppm. At the same time graphitic BC contents determined by thermal oxidation were 23 to 355% greater in Anthrosols than adjacent soils. We conclude that BC contributed more to total organic C contents in the studied Anthrosols than in adjacent soils. Therefore, these pairs of Anthrosols and adjacent soils provided an opportunity for examining the effects of BC on CEC of soils with identical mineralogy and climate.

Cation Exchange Capacity

Cation exchange capacity of Anthrosols and adjacent soils were plotted against soil organic C for all horizons at each site (Fig. 2). Cation exchange capacities per unit soil C were up to 1.9 times higher in Anthrosols with high BC than in the adjacent soils. Linear regressions indicated a greater slope of the correlation between CEC and soil organic C, with 8.6 for Anthrosols and 2.8

Table 2. Black C concentrations and physical properties of BC-rich Anthrosols and adjacent soils in the central Amazon.

Site	Type	Graphitic BC [†]		Aromat.	CEC [§]	ECEC [¶]	SSA [#]	SSA-clay	Charge Density	C _{OM} ^{††}	CEC _{OM} ^{‡‡}	ΔCEC ^{§§}	CEC _{OM} ^{¶¶}
		— % of total C —	Char-BC [‡]										
HAT	Anthrosol	5.82	nd##	0.51	211.3	213.0	7.2	90.8	29.34	7.4	188.1	11.0	25.4
	Adjacent soil	2.87	nd	0.23	88.4	23.0	17.2	45.5	5.14	2.6	59.9	32.2	23.0
LG	Anthrosol	2.32	51.4	0.31	222.4	158.7	24.4	107.3	9.11	7.2	191.6	13.8	26.6
	Adjacent soil	1.88	<	0.13	59.2	22.3	14.9	56.9	3.97	2.4	56.4	4.6	23.5
ACU	Anthrosol	5.71	nd	0.40	56.3	11.5	6.3	74.3	8.93	0.8	45.7	18.7	57.1
	Adjacent soil	2.41	nd	0.26	52.0	15.1	4.7	55.2	11.05	1.3	27.9	46.2	21.5
DS	Anthrosol	3.23	nd	0.50	26.7	5.1	0.5	288.3	53.42	0.4	19.4	27.4	48.5
	Adjacent soil	0.71	nd	0.15	80.8	7.9	0.1	3.6	o.b.	0.6	18.6	78.0	31.0

[†] Graphitic BC determined by thermal oxidation.

[‡] Char-BC determined by UV oxidation after HF treatment and ¹³C CP/MAS NMR spectroscopy.

[§] Potential cation exchange capacity.

[¶] Effective cation exchange capacity.

[#] SSA: specific surface area.

^{††} Soil organic C concentration after treatment with H₂O₂.

^{‡‡} Potential cation exchange capacity after treatment with H₂O₂.

^{§§} Difference between potential CEC before and after treatment with H₂O₂.

^{¶¶} Potential CEC per unit organic C after treatment with H₂O₂.

nd not determined; < below detection limit of 1.5%.

for adjacent soils. This trend is in agreement with results by Sombroek et al. (1993) for Anthrosols with high BC contents in comparison to adjacent forest soils (shaded dots in Fig. 2).

To estimate the contribution of BC to total CEC, CEC was measured for soil samples after removing non-BC using peroxide. Upon peroxide treatment, CEC per unit C was 10 to 166% greater in Anthrosols than adjacent soils (Table 2). The CEC per unit soil decreased much more in adjacent soils (32–78%) than in Anthrosols (11–27%) apart from the LG site. The exception at the LG site can be explained by the greater SOM contents of the Anthrosol than the adjacent soil at LG, which may have resulted in a lower efficiency of peroxide to remove organic C (Leifeld and Kögel-Knabner, 2001).

Although hydrogen peroxide reportedly has a low removal efficiency compared with NaOCl and Na₂S₂O₈ (Mikutta et al., 2005), residual organic C is largely comprised of refractory SOM (mainly pyrogenic materials and aliphatic compounds). It was found that peroxide-resistant SOM is thermally more stable than total SOM (Plante et al., 2005). Plante et al. (2005) also suggested that peroxide-resistant SOM may be composed of an inert pool of SOM with properties indicating the presence of BC. Therefore, we consider this portion of residual C in Anthrosols as BC in the sense of being resistant to oxidation by peroxide, whereas this recalcitrant fraction may largely consist of non-BC in adjacent soils. Peroxide may have not only removed non-BC in the Anthrosols, but also oxidized aromatic C on BC

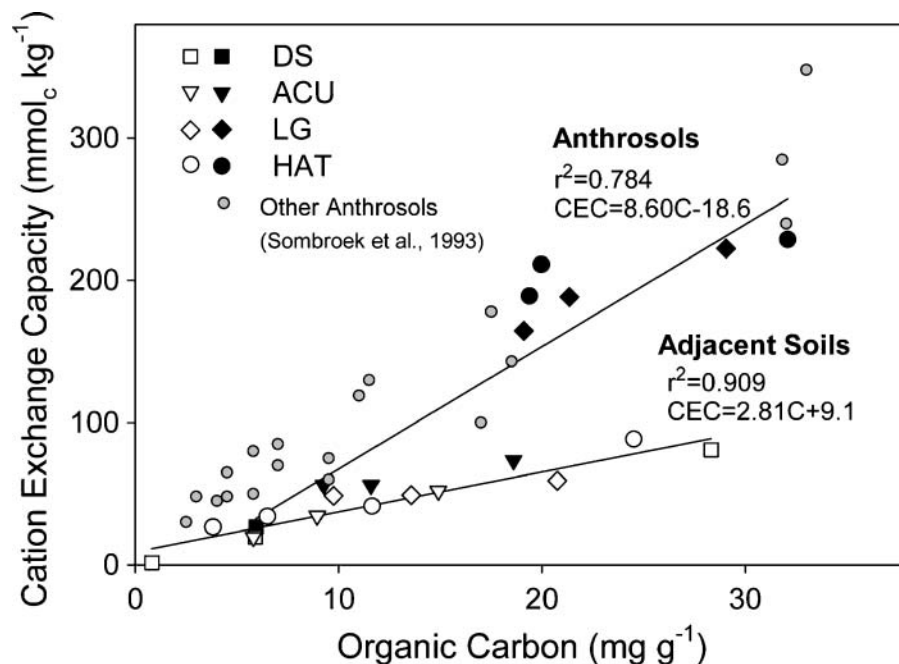


Fig. 2. Potential cation exchange capacity (CEC) determined with NH₄-Ac buffered at pH 7 as influenced by organic C for Anthrosols (filled symbols) in comparison to adjacent soils (open symbols) of similar clay mineralogy at four different sites and different soil horizons. Regression only for soils in our study, excluding Anthrosols from Sombroek et al. (1993).

surfaces to form carboxylic groups that could result in the formation of CEC (Mikutta et al., 2005), as shown for HNO₃ oxidation of fresh eucalyptus charcoal (Trompowsky et al., 2005). Therefore, it cannot be excluded that the CEC of peroxide-treated Anthrosols is the CEC that can be created after oxidation of surface functional groups of BC particles. This should be evaluated in future experiments.

Soil Surface Area and Charge Density

The SSA per unit clay found for adjacent soils in our study was similar to values reported by others (Table 2). For example, Chorover and Sposito (1995) found values

of 65 to 104 m² g⁻¹ clay using the ethylene-glycol-monooethyl ether adsorption method for the clay fraction of several kaolinitic soils. Anthrosols had up to 4.8 times higher SSA than adjacent soils (except HAT with 42% less SSA) (Table 2). After normalization for different clay contents, the difference was even more striking with SSA being relatively low for adjacent soils (≤ 56.9 m² g⁻¹ clay), but very high for Anthrosols (≥ 74.3 m² g⁻¹ clay). Such differences between Anthrosols and adjacent soils suggested that the BC had a large surface area.

Charge density calculated from dividing CEC by the SSA (Table 2) was about two times higher in Anthrosols than adjacent soils, except at those sites that had very low SSA in general, which may have led to inaccuracies

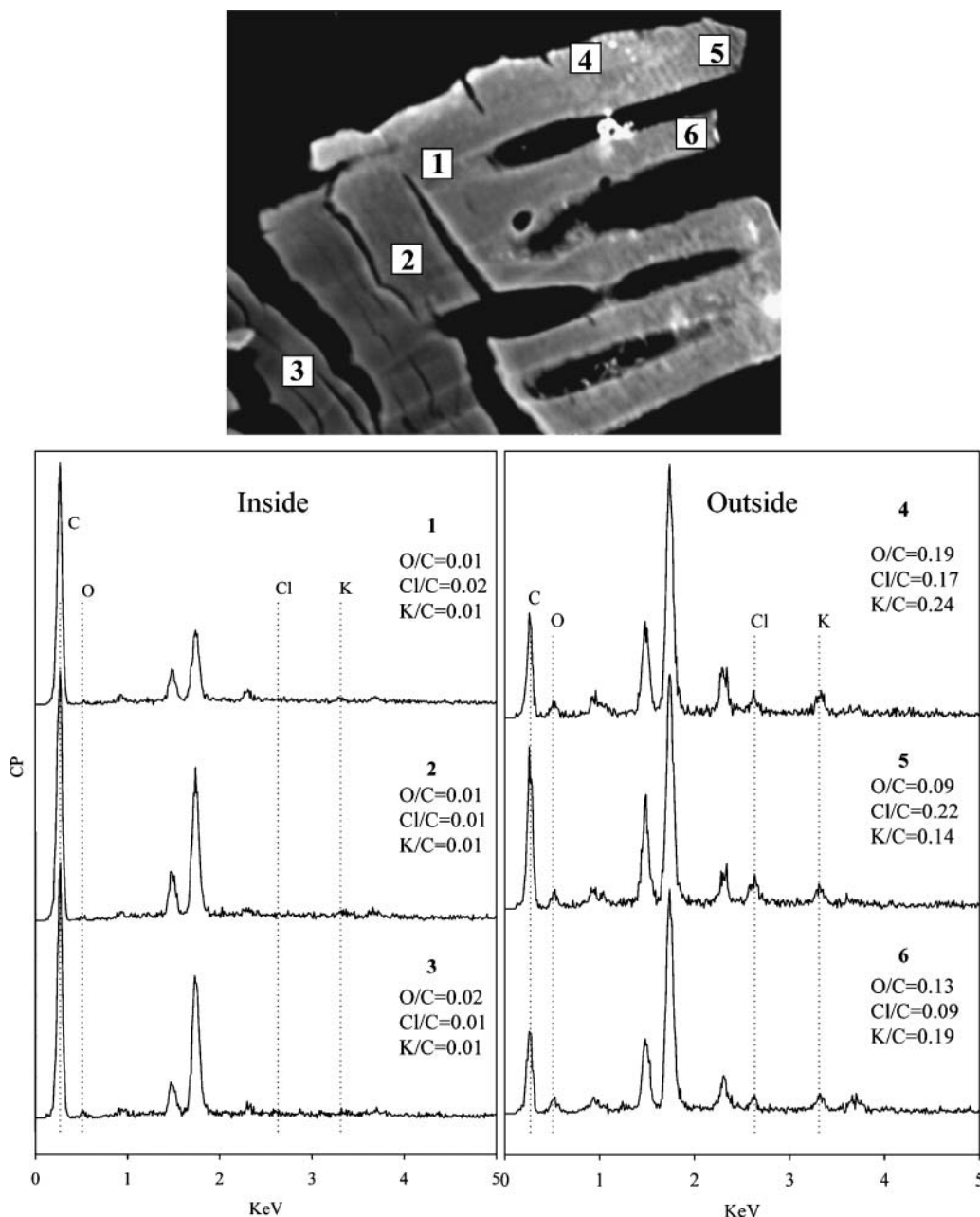


Fig. 3. Microprobe elemental analysis spectra for a BC thin section (ACU II BC particle). Numbers 1, 2, 3 indicate the measured spots in the interior of the BC particle ('inside'), 4, 5, 6 indicate those toward the surface of the BC particle ('outside').

in determining SSA. Since kaolinitic clays negligibly contribute to surface charge in most Amazonian upland soils (Anderson and Sposito, 1991), most of the exchange capacity is created by organic matter (Sombroek, 1966). In general, surface chemical properties are greatly affected by the relative contents of mineral and organic soil constituents (Marcano-Martinez and McBride, 1989). At our study site, BC was found to be very effective in contributing to CEC. Therefore, the high CEC observed in soils that are rich in BC such as the studied Anthrosols was a function of both a high charge density on BC surfaces and a high surface area of BC particles.

Surface Oxidation of Black Carbon

If BC not only contributes significantly to the surface area of soils but also exhibits a larger CEC per unit surface area as well as per unit mass, questions arise whether surface oxidation of BC particles was responsible for the observed increase in CEC. Microprobe equipped with elemental mapping function was explored to measure the distribution of elements across BC sections (Fig. 3). Overall, a low O/C ratio (0.00–0.19) was observed for the entire particle, which confirmed a high aromaticity of the studied BC particle. Yet a higher O/C (0.09–0.19) was observed near the surface than in the interior (0.01–0.02) of the BC particle obtained by point spectra observation, which indicated a higher level of oxidation close to the surface of the BC particle compared with its center. A greater O/C ratio near BC surfaces was also noted by Brodowski et al. (2005) using energy-dispersive X-ray spectroscopy. Notably, a higher concentration of Cl and K was also observed near the surface of our BC particle, which could be discriminated by peak appearance and Cl/C and K/C ratios. Near the surface of the BC particle, Cl/C and K/C ratios were higher (0.09–0.22 and 0.19–0.24, respectively) than those at the inside (<0.02 and 0.01, respectively). The occurrence of both anions and cations on the surface of the studied BC particle suggested nutrient adsorption to the BC particle.

Carbon Forms in Black Carbon

Synchrotron-based NEXAFS spectroscopy was used to investigate the C forms in BC compared with other forms of C in soil. Absorption peaks at certain energy levels were assigned to different functional groups according to published data (Table 3). Aromatic-C peaks are typically found in the energy range of 284.9 to 285.5 eV. In our study, large and well-defined peaks were found at 284.8 to 285.1 eV in all BC samples, whereas microorganisms and humic substances extracts showed comparatively small peaks at slightly higher energy levels of 285.3 to 285.4 eV. Characteristic for BC was also a peak in the energy range of 285.8 to 286.4 eV that is commonly attributed to unsaturated/carbonyl-substituted aromatic-C (Table 3), which was discussed in detail by Lehmann et al. (2005). Within that energy range our BC samples showed distinct peaks at 285.9 to 286.4 eV similar to fresh BC (Table 3), while humic substances or microorganisms did not show peaks at these energy levels. In some areas of BC particles phenol-C and ketone C = O (286.6–286.8 eV) were found (Table 3; Fig. 4 and 5), which was very distinct for humic substances extracts (Fig. 6 and Scheinost et al., 2001; Schäfer et al., 2003; Solomon et al., 2005) but not for microorganisms (Fig. 6). Aliphatic and transitional aromatic C-OH functional groups (287.1–287.4 eV) only contributed as a trace component to overall spectra of all studied organic compounds. In contrast, all organic materials showed a distinct and strong peak in the energy range of carboxyl-C (287.7–288.6) with peak positions clustering around 288.5–288.7 eV (Table 3). Carbonyl-C and alcohols at 289.6 eV were only resolved clearly in spectra obtained from microorganisms (Fig. 6; Table 3). In comparison, the studied clay particle showed no or only traces of peaks with a typical ‘flat’ spectrum and high optical density below the K-edge of C (Fig. 6). These results demonstrated that C forms in BC were distinct from other organic materials in the studied soils and could be distinguished using NEXAFS. The combination of NEXAFS with STXM will then allow the study of the

Table 3. Approximate energy ranges (eV) for primary absorption peak assignments at the carbon 1s K-edge and identified peaks at different energy levels for two black C (BC) particles (apart from DS with only one BC particle) from selected horizons of Anthrosols (corresponding to Table 1), and non-BC including clay, bacteria, fungi, and humic substance extract (see methods for description of sample details).

	Protonated/alkylated aromatic-C	Unsaturated/Carbonyl substituted aromatic-C	Phenol-C Ketone C=O	Aliphatic-C, aromatic C-OH	Carboxyl-C, CH ₃ , CH ₂ , CH	Alcohol, carbonyl-C	Carbonate
BC HAT I	284.9–285.5 [†]	285.8–286.4 [†]	286.6–286.8 [†]	287.1–287.4 [†]	287.7–288.6 [†]	289.3–289.6 [†]	290.3–290.6 [†]
BC HAT II	284.8	286.1	–	–	288.5–288.6	–	–
BC LG I	285.0	286.2–286.7	286.7	trace	288.6–288.7	–	–
BC LG II	285.0	286.3	–	trace	288.5	–	–
BC ACU I	284.9–285.0 [‡]	286.3–286.4	trace [§]	trace	288.6–288.7	–	–
BC ACU II	284.8–284.9	286.1–286.4	–	–	288.5	–	–
BC DS	285.0–285.1	286.2–286.3	–	trace	288.3–288.4	–	–
BC DS	284.9–285.1	286.1	–	trace	288.6–288.7	–	–
BC [¶] (charcoal)	284.9	286.2	–	trace	trace	–	trace
Clay ACU	–	–	–	–	–	–	trace
Bacteria	285.3	–	–	trace	288.4	289.6	–
Fungi	285.4	–	–	trace	288.7	289.6	291.1
Humic Substance	285.3	–	286.8	–	288.7	–	–

[†] Sources: Hitchcock et al. (1986, 1992), Hitchcock and Ishii (1987), Hitchcock and Stöhr (1987), Francis and Hitchcock (1992), Cody et al. (1998), Urquhart and Ade (2002), Brandes et al. (2004) and Lehmann et al. (2005).

[‡] A range is given for BC samples that all have multiple areas (A, B, C, see Fig. 4 and 5).

[§] Trace: small, not significant or overlapping.

[¶] From Lehmann et al. (2005).

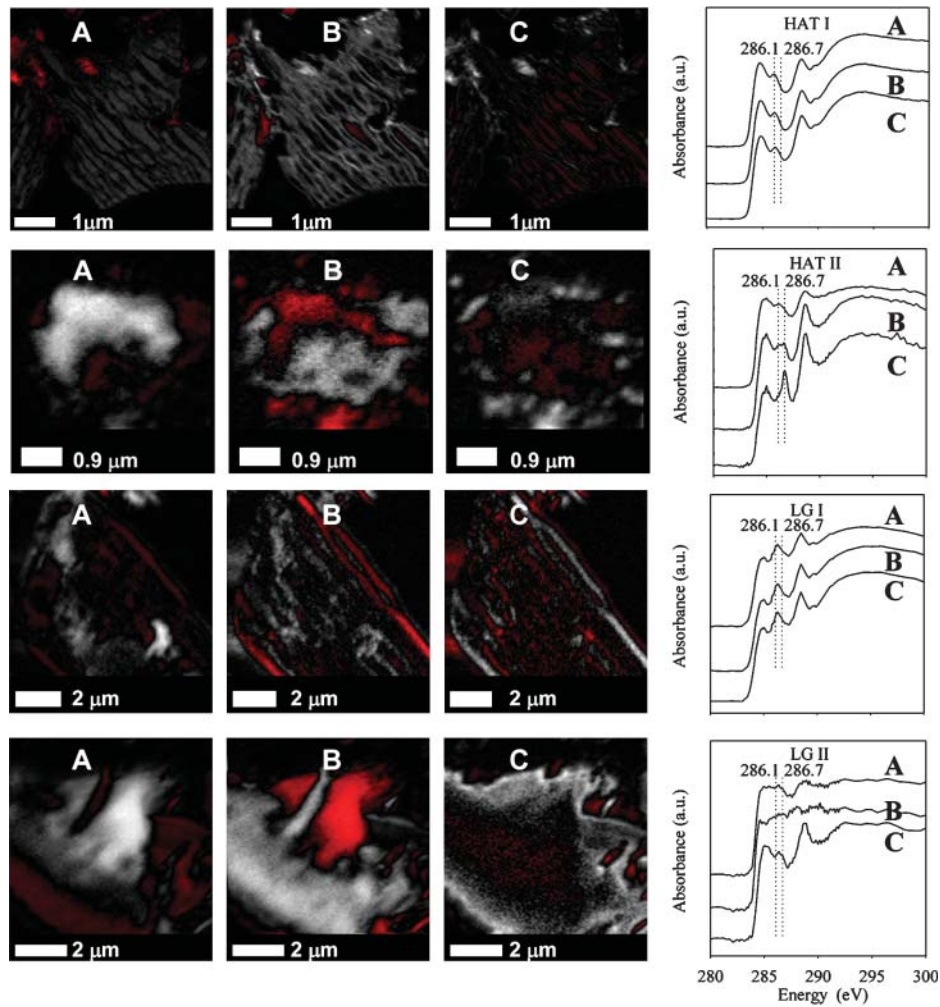


Fig. 4. Carbon NEXAFS target maps and fitted spectra for BC thin sections in HAT and LG sites. A = core/inside; B = intermediate layer; C = close to the surface. Two BC particles denoted with Latin numbers from one horizon described in Table 1.

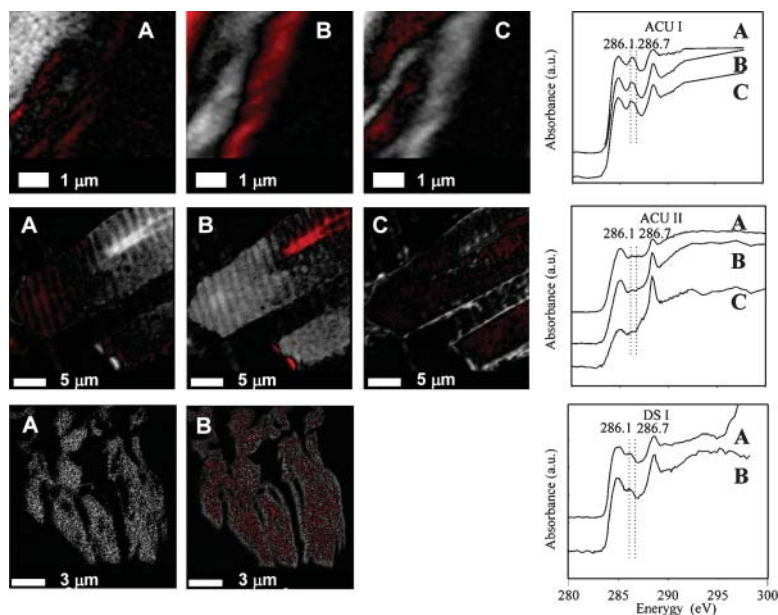


Fig. 5. Carbon NEXAFS target maps and fitted spectra for BC thin sections in ACU and DS sites. A = core/inside; B = intermediate layer; C = close to the surface. Two (ACU) and one (DS) BC particle denoted with Latin numbers from one horizon described in Table 1.

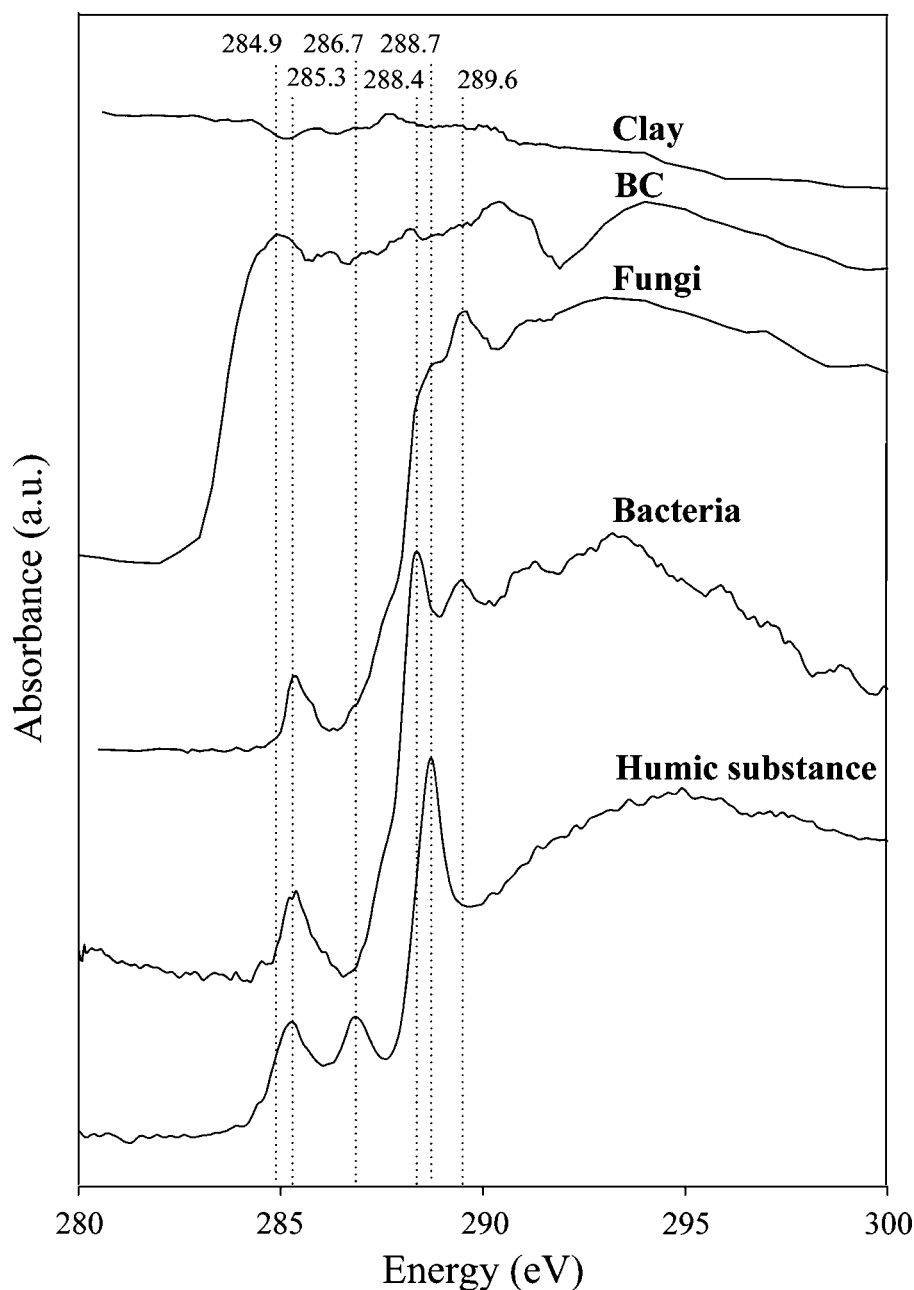


Fig. 6. Carbon NEXAFS spectra for a clay thin section from ACU, isolated fungi and bacteria, humic substance representing non-BC obtained from adjacent soil at HAT, in comparison to a BC sample (fresh charcoal from Lehmann et al., 2005).

spatial distribution of C forms in BC and the extent and sources of surface oxidation.

Process of Surface Oxidation of Black Carbon

To understand the mechanism of surface oxidation of BC, spatial analyses of C forms obtained by a combination of NEXAFS with STXM were performed using principle component analyses (Lerotic et al., 2004; Lehmann et al., 2005). The chemical signatures in cross-sections of BC particles were not homogeneous (Fig. 4 and 5). The most distinct change was the progressive increase of oxidized C, especially carboxyl-C, and the decrease in aromatic-C. In addition to the changes in relative pro-

portions of functional groups, also more subtle changes in chemical forms and unique structures could be observed. Notably the peaks at the energy region of aromatic-C were relatively broad for BC, indicating a low order structure and heterogeneous nature of the BC. This was more pronounced in the interior areas than close to the surface of BC particles. The most important difference in C forms was the shift of the peak from the region of unsaturated C (286.1 eV) in the interior and intermediate areas of BC particles (maps and spectra A and B in Fig. 4 and 5) to the region of phenol-C (286.7 eV) in the outer areas (maps and spectra C) for most particles. This result confirms the observations by Lehmann et al. (2005) based on the analysis of a single BC particle (analyzed using a different

procedure at HAT II), although the extent of the peak shift varies between particles. Aliphatic and transitional aromatic C-OH functional groups (287.1–287.4 eV) were only clearly distinguishable in spectra that described outer areas (maps C) of the BC particles.

Spectra of the interior of BC particles (maps A; Fig. 4 and 5) closely resembled those obtained for charcoal (Fig. 6). In all studied particles, this largely unaltered core was surrounded by more oxidized organic matter (maps B) that is most likely of the same origin as the more aromatic BC core. Therefore, oxidation of BC particles occurred and could contribute to the high charge density on surfaces of BC particles. In addition, outer areas (maps C) were in most cases not only more oxidized than the two inner areas (maps A and B), but in several particles they also showed distinct peak shifts such as the disappearance of the peak at 286.1 eV characteristic of BC and the appearance of the peak at 286.7 eV characteristic of humic substances. Following the hypothesis developed by Lehmann et al. (2005), this change would indicate that this type of outer area is not oxidized BC but adsorbed non-BC. Therefore, both adsorption of non-BC as well as oxidation of the BC itself led to oxidized surfaces which can be held responsible for the high CEC associated with BC.

While slight to clear shifts from 286.1 to 286.7 eV were visible in several BC particles (HAT I, HAT II, LG II, ACU II), others did not show this shift (LG I, ACU I) or did not even show a third distinct region (DS I) (Fig. 4 and 5). The spectral signature of the described peak shift is only one criterion that can be used for answering the question whether adsorption took place and to what extent. Also the spatial distribution of C forms can be used to distinguish the two processes of either oxidation of the BC particle itself or adsorption of non-BC to BC particle surfaces. Some BC particles clearly showed a discontinuous and spotty distribution of the outer region (HAT I, HAT II, ACU II) that may indicate adsorption of organic matter. In some cases, however, the outer region (map C for example in LG II and ACU I, or map B in DS I) showed spatial attributes that appeared to indicate oxidation of BC particles rather than adsorption.

The adsorbed organic matter could originate from either plant material or microbial metabolites. The source of this adsorbed C could not be fully resolved, since the isolation of single BC particles from soil did not allow us to evaluate the C forms in and around the BC particles in the context of the soil matrix and microbial population. In some particles, the weak or nonexistent changes in the spectral characteristics of the outer areas at 286.1 eV may indicate that the adsorbed organic matter did not originate from non-BC but from oxidized BC. Such areas still showed the spatial attributes of adsorbed organic matter (non-continuous and spotty rather than a thin layer), but at the same time the chemical characteristics of BC (peak at 286.1 eV and no change toward higher energy). In these cases, oxidized BC may have been sloughed off BC particles and re-adsorbed to the same or other BC particles as indicated by the similar spectral characteristics to BC but morphological characteristics of adsorbed organic matter.

CONCLUSIONS

Oxidized functional groups on BC particles originated either from oxidation of BC itself or from adsorption of partially oxidized BC or non-BC materials. Evidence was provided from changes in chemical characteristics (shift of the peak at 286.1 eV to a higher energy) and from spatial attributes of outer regions of the BC particles. This surface oxidation led to a higher CEC per unit C as well as to a higher charge density in BC-rich Anthrosols compared to BC-poor adjacent soils. Additionally, the Anthrosols showed a higher surface area due to their higher BC concentrations. Therefore, BC was more efficient in providing CEC and cation retention than non-BC in the studied soils. Further research is warranted that examines the oxidation of BC under different temperature and moisture regimes and the interactions of BC surfaces with clay particles and aggregation.

ACKNOWLEDGMENTS

This project was funded by the Division of Environmental Biology of the National Science Foundation under contract DEB-0425995. The NEXAFS spectra were obtained at the National Synchrotron Light Source (NSLS), Brookhaven National Laboratory, at the beamline X-1A1 developed by the group of Janos Kirz and Chris Jacobsen at SUNY Stony Brook, with support from the Office of Biological and Environmental Research, U.S. DoE under contract DE-FG02-89ER60858, and the NSF under grants DBI-9605045 and ECS-9510499. Many thanks to Murray McBride for insightful discussion, to Fernando Costa and Manuel Arroyo-Kalin for help with sampling, to Sue Wirick for guiding us through the X-ray measurements, to John Hunt for great technical support for the microprobe measurement, and to Yuanming Zhang and Scott Warren for invaluable help with sectioning and surface area measurements, respectively.

REFERENCES

- Accardi-Dey, A., and P.M. Gschwend. 2002. Assessing the combined roles of natural organic matter and black carbon as sorbents in sediments. *Environ. Sci. Technol.* 36:21–29.
- Anderson, S.J., and G. Sposito. 1991. Cesium-adsorption method for measuring accessible structural surface-charge. *Soil Sci. Soc. Am. J.* 55:1569–1576.
- Braida, W.J., J.J. Pignatello, Y.F. Lu, P.I. Ravikovitch, A.V. Neimark, and B.S. Xing. 2003. Sorption hysteresis of benzene in charcoal particles. *Environ. Sci. Technol.* 37:409–417.
- Brandes, J.A., C. Lee, S. Wakeham, M. Peterson, C. Jacobsen, S. Wirick, and G. Cody. 2004. Examining marine particulate organic matter at sub-micron scales using scanning transmission x-ray microscopy and carbon x-ray absorption near-edge structure spectroscopy. *Mar. Chem.* 92:107–121.
- Brodowski, S., W. Amelung, L. Haumaier, C. Abetz, and W. Zech. 2005. Morphological and chemical properties of black carbon in physical soil fractions as revealed by scanning electron microscopy and energy-dispersive x-ray spectroscopy. *Geoderma* 128:116–129.
- Chorover, J., and G. Sposito. 1995. Surface charge characteristics of kaolinitic tropical soils. *Geochim. Cosmochim. Acta* 59:875–884.
- Cody, G.D., H. Ade, S. Wirick, G.D. Mitchell, and A. Davis. 1998. Determination of chemical-structural changes in vitrinite accompanying luminescence alteration using C-NEXAFS analysis. *Org. Geochem.* 28:441–455.
- Fernandes, M.B., J.O. Skjemstad, B.B. Johnson, J.D. Wells, and P. Brooks. 2003. Characterization of carbonaceous combustion residues. I. Morphological, elemental and spectroscopic features. *Chemosphere* 51:785–795.

- Francis, J.T., and A.P. Hitchcock. 1992. Inner-shell spectroscopy of para-benzoquinone, hydroquinone, and phenol: Distinguishing quinoid and benzenoid structures. *J. Phys. Chem.* 96:6598–6610.
- Gee, G.W., and D. Or. 2002. Particle-size analysis. p. 255–293. *In* J.H. Dane, and G.C. Topp (ed.) *Methods of soil analysis. Part 4. SSSA Book Ser. 5. SSSA, Madison, WI.*
- Gelinas, Y., K.M. Prentice, J.A. Baldock, and J.I. Hedges. 2001. An improved thermal oxidation method for the quantification of soot/graphitic black carbon in sediments and soils. *Environ. Sci. Technol.* 35:3519–3525.
- Ghosh, U., J.S. Gilette, R.G. Luthy, and R.N. Zare. 2000. Microscale location, characterization, and association of polycyclic aromatic hydrocarbons on harbor sediment particles. *Environ. Sci. Technol.* 34:1729–1736.
- Gillman, G.P., and E.A. Sumpter. 1986. Modification to the compulsive exchange method for measuring exchange characteristics of soils. *Austr. J. Soil Res.* 24:61–66.
- Glaser, B., L. Haumaier, G. Guggenberger, and W. Zech. 2001. The 'Terra Preta' phenomenon: A model for sustainable agriculture in the humid tropics. *Naturwissenschaften* 88:37–41.
- Glaser, B., G. Guggenberger, W. Zech, and M.L. Rivo. 2003. Soil organic matter stability in Amazonian Dark Earths. p. 141–158. *In* J. Lehmann et al. (ed.) *Amazonian dark earths: Origin, properties, management.* Kluwer Academic Publishers, Dordrecht, The Netherlands.
- Gustafsson, O., F. Haghseta, C. Chan, J. MacFarlane, and P.M. Gschwend. 1997. Quantification of the dilute sedimentary soot phase: Implications for PAH speciation and bioavailability. *Environ. Sci. Technol.* 31:203–209.
- Hendershot, W.H., and M. Duquette. 1986. A simple barium-chloride method for determining cation-exchange capacity and exchangeable cations. *Soil Sci. Soc. Am. J.* 50:605–608.
- Hitchcock, A.P., and I. Ishii. 1987. Carbon K-shell excitation-spectra of linear and branched alkanes. *J. Electron Spectr. Rel. Phenom.* 42:11–26.
- Hitchcock, A.P., and J. Stöhr. 1987. K-shell shape resonances and intramolecular bond lengths—comments on the relationship between shape resonances and bond lengths. *J. Chem. Phys.* 87:3253–3255.
- Hitchcock, A.P., J.A. Horsley, and J. Stöhr. 1986. Inner-shell excitation of thiophene and thiolane—gas, solid, and monolayer states. *J. Chem. Phys.* 85:4835–4848.
- Hitchcock, A.P., S.G. Urquhart, and E.G. Rightor. 1992. Inner-shell spectroscopy of benzaldehyde, terephthalaldehyde, ethyl benzoate, terephthaloyl chloride, and phosgene—models for core excitation of poly(ethylene-terephthalate). *J. Phys. Chem.* 96:8736–8750.
- Holmgren, G.G.S., R.L. Juve, and R.C. Geschwender. 1977. A mechanically controlled variable rate leaching device. *Soil Sci. Soc. Am. J.* 41:1207–1208.
- Kuhlbusch, T.A.J., M.O. Andreae, H. Cachier, J.G. Goldammer, J.P. Lacaux, R. Shea, and P.J. Crutzen. 1996. Black carbon formation by savanna fires: Measurements and implications for the global carbon cycle. *J. Geophys. Res. Atmos.* 101:23651–23665.
- Lehmann, J., M.S. Cravo, J.L.V. Macedo, A. Moreira, and G. Schroth. 2001. Phosphorus management for perennial crops in central Amazonian upland soils. *Plant Soil* 237:309–319.
- Lehmann, J., D.C. Kern, L.A. German, J. McCann, G.C. Martins, and A. Moreira. 2003a. Soil fertility and production potential. p. 105–124. *In* J. Lehmann et al. (ed.) *Amazonian dark earths: Origin, properties, management.* Kluwer Academic Publishers, Dordrecht, The Netherlands.
- Lehmann, J., J.P. da Silva, C. Steiner, T. Nehls, W. Zech, and B. Glaser. 2003b. Nutrient availability and leaching in an archaeological Anthrosol and a Ferralsol of the Central Amazon basin: Fertilizer, manure and charcoal amendments. *Plant Soil* 249:343–357.
- Lehmann, J., B.Q. Liang, D. Solomon, M. Lerotic, F. Luizao, J. Kinyangi, T. Schäfer, S. Wirick, and C. Jacobsen. 2005. Near-edge x-ray absorption fine structure (NEXAFS) spectroscopy for mapping nano-scale distribution of organic carbon forms in soil: Application to black carbon particles. *Global Biogeochem. Cycles* 19:1013.
- Leifeld, J., and I. Kögel-Knabner. 2001. Organic carbon and nitrogen in fine soil fractions after treatment with hydrogen peroxide. *Soil Biol. Biochem.* 33:2155–2158.
- Lerotic, M., C. Jacobsen, T. Schäfer, and S. Vogt. 2004. Cluster analysis of soft X-ray spectromicroscopy data. *Ultramicroscopy* 100:35–57.
- Lima, H.N., C.E.R. Schaefer, J.W.V. Mello, R.J. Gilkes, and J.C. Ker. 2002. Pedogenesis and pre-Colombian land use of "Terra Preta Anthrosols" ("Indian black earth") of Western Amazonia. *Geoderma* 110:1–17.
- Marcano-Martinez, E., and M.B. McBride. 1989. Calcium and sulfate retention by two Oxisols of the Brazilian cerrado. *Soil Sci. Soc. Am. J.* 53:63–69.
- Masiello, C.A. 2004. New directions in black carbon organic geochemistry. *Mar. Chem.* 92:201–213.
- Masiello, C.A., E.R.M. Druffel, and L.A. Currie. 2002. Radiocarbon measurements of black carbon in aerosols and ocean sediments. *Geochim. Cosmochim. Acta* 66:1025–1036.
- McCann, J.M., W.I. Woods, and D.W. Meyer. 2001. Organic matter and anthrosols in Amazonia: Interpreting the Amerindian legacy. p. 180–189. *In* R.M. Rees et al. (ed.) *Sustainable management of soil organic matter.* CAB International, Wallingford, UK.
- Mikutta, R., M. Kleber, K. Kaiser, and R. John. 2005. Review: Organic matter removal from soils using hydrogen peroxide, sodium hypochloride, and disodium perodisulfate. *Soil Sci. Soc. Am. J.* 69:120–135.
- Neves, E.G., J.B. Petersen, R.N. Bartone, and C.A.D. Silva. 2003. Historical and socio-cultural origins of Amazonian Dark Earths, p. 29–50. *In* J. Lehmann et al. (ed.) *Amazonian dark earths: Origin, properties, management.* Kluwer Academic Publishers, Dordrecht, The Netherlands.
- Palotas, A.B., L.C. Rainey, C.J. Feldermann, A.F. Sarofim, and J.B. van der Sande. 1996. Soot morphology: An application of image analysis in high-resolution transmission electron microscopy. *Microscopy Res. Technol.* 33:266–278.
- Pennell, K.D. 2002. Specific surface area. p. 295–315. *In* G.C. Topp, and J.H. Dane (ed.) *Methods of soil analysis. Soil Book ser. No. 5. SSSA, Madison, WI.*
- Petersen, J., E.G. Neves, and M.J. Heckenberger. 2001. Gift from the past: Terra preta and prehistoric amerindian occupation in Amazonia. p. 86–105. *In* C. McEwan (ed.) *Unknown Amazonia.* British Museum, London.
- Plante, A.F., M. Pernes, and C. Chenu. 2005. Changes in clay-associated organic matter quality in a C depletion sequence as measured by differential thermal analyses. *Geoderma* 129:186–199.
- Rothe, J., J. Hormes, C. Schild, and B. Pennemann. 2000. X-ray absorption spectroscopy investigation of the activation process of Raney Nickel catalysts. *J. Catal.* 191:294–300.
- Schafer, T., N. Hertkorn, R. Artinger, F. Claret, and A. Bauer. 2003. Functional group analysis of natural organic colloids and clay association kinetics using C(1s) spectromicroscopy. *J. Phys. France* 104: 409–412.
- Scheinost, A.C., R. Kretzschmar, I. Christl, and C. Jacobsen. 2001. Carbon group chemistry of humic and fulvic acid: A comparison of C-1s NEXAFS and ¹³C-NMR spectroscopies. p. 39–47. *In* E.A. Ghabbour and G. Davies (ed.) *Humic substances: Structures, models and functions.* Royal Society of Chemistry, Gateshead, UK.
- Schmidt, M.W.I., and A.G. Noack. 2000. Black carbon in soils and sediments: Analysis, distribution, implications, and current challenges. *Global Biogeochem. Cycles* 14:777–793.
- Schmidt, M.W.I., J.O. Skjemstad, E. Gehrt, and I. Kögel-Knabner. 1999. Charred organic carbon in German chernozemic soils. *Eur. J. Soil Sci.* 50:351–365.
- Schmidt, M.W.I., J.O. Skjemstad, and C. Jäger. 2002. Carbon isotope geochemistry and nanomorphology of soil black carbon: Black chernozemic soils in central Europe originate from ancient biomass burning. *Global Biogeochem. Cycles* 16:1123.
- Skjemstad, J.O., P. Clarke, J.A. Taylor, J.M. Oades, and S.G. McClure. 1996. The chemistry and nature of protected carbon in soil. *Austr. J. Soil Res.* 34:251–271.
- Skjemstad, J.O., J.A. Taylor, and R.J. Smernik. 1999. Estimation of charcoal (char) in soils. *Commun. Soil Sci. Plant Anal.* 30:2283–2298.
- Smith, N.J.H. 1980. Anthrosols and human carrying capacity in Amazonia. *Ann. Assoc. Am. Geogr.* 70:553–566.
- Solomon, D., J. Lehmann, J. Kinyangi, B.Q. Liang, and T. Schäfer. 2005. Carbon K-edge NEXAFS and FTIR-ATR spectroscopic investigation of organic carbon speciation in soils. *Soil Sci. Soc. Am. J.* 69:107–119.
- Sombroek, W.G. 1966. Amazon Soils: A reconnaissance of the soils of the Brazilian Amazon Region. Wageningen: Center for Agricultural Publications and Documentation.
- Sombroek, W.G., F.O. Nachtergaele, and A. Hebel. 1993. Amounts,

- dynamics and sequestering of carbon in tropical and subtropical soils. *Ambio* 22:417–426.
- Sombroek, W.G. 2001. Spatial and temporal patterns of Amazon rainfall. *Ambio* 30:388–396.
- Stoffyn-Egli, P., T.M. Potter, J.D. Leonard, and R. Pocklington. 1997. The identification of black carbon particles with the analytical scanning electron microscope: Methods and initial results. *Sci. Total Environ.* 198:211–223.
- Sumner, M.E., and W.P. Miller. 1996. Cation exchange capacity and exchange coefficients, p. 1201–1229. *In* D.L. Sparks (ed.) *Methods of soil analysis*. SSSA Book Ser. No. 5. SSSA and ASA, Madison, WI.
- Trompowsky, P.M., V.M. Benites, B.E. Madari, A.S. Pimenta, W.C. Hockaday, and P.G. Hatcher. 2005. Characterization of humic like substances obtained by chemical oxidation of eucalyptus charcoal. *Org. Geochem.* 36:1480–1489.
- Urquhart, S.G., and H. Ade. 2002. Trends in the carbonyl core (C 1s, O 1s) \rightarrow $\pi_{C=O}$ transition in the near-edge x-ray absorption fine structure spectra of organic molecules. *J. Phys. Chem. B* 106:8531–8538.
- USDA. 1999. *Soil Taxonomy: A basic system of soil classification for making and interpreting soil surveys*. *In* NRCS (ed.) 2nd ed. USDA, Washington, DC.
- Whittig, L.D., and W.R. Allardice. 1986. X-ray diffraction techniques, p. 331–362. *In* A. Klute (ed.) *Methods of soil analysis*. Part 1. *Agron. Monogr.* No. 9 ASA and SSSA, Madison, WI.